Available online at www.sciencedirect.com
SCIENCE DIRECT®
automatica
Automatica 41 (2005) 289–298
www.elsevier.com/locate/automatica

Brief paper

Adaptive maneuvering, with experiments, for a model ship in a marine control laboratory☆

Roger Skjetne[a,*], Thor I. Fossen[a,b], Petar V. Kokotović[c]

[a]*Department of Engineering Cybernetics, Norwegian University of Science and Technology (NTNU), NO-7491 Trondheim, Norway*
[b]*Centre for Ships and Ocean Structures (CeSOS), Norwegian University of Science and Technology (NTNU), NO-7491 Trondheim, Norway*
[c]*Center for Control Engineering and Computation (CCEC), University of California, Santa Barbara (UCSB), CA 93106, USA*

Received 12 November 2003; received in revised form 25 September 2004; accepted 20 October 2004
Available online 10 December 2004

Abstract

The maneuvering problem involves two tasks. The first, called the geometric task, is to force the system output to converge to a desired path continuously parametrized by a scalar θ. The second task, called the dynamic task, is to satisfy a desired dynamic behavior along the path. In this paper, this dynamic behavior is further specified as a speed assignment for $\theta(t)$. While the main concern is to satisfy the geometric task, the dynamic task ensures that the system output follows the path with the desired speed. An adaptive recursive design technique is developed for a parametrically uncertain nonlinear plant describing the dynamics of a ship. First the geometric part of the problem is solved. Then an update law is constructed that bridges the geometric design with the dynamic task. The design procedure is performed and tested by several experiments for a model ship in a marine control laboratory.

Keywords: Maneuvering; Path following; Tracking; Backstepping; Adaptive control; Marine vessels; Ship experiments

1. Introduction

The maneuvering problem formulation was motivated by applications in which steering an object along a desired path is more important than the speed assignment along the path, which can be left free for a human operator, or solved as a separate task. Applications of this type are described by Micaelli and Samson (1993), Hauser and Hindman (1995, 1997), Encarnação and Pascoal (2001), Pettersen and Lefeber (2001), Al-Hiddabi and McClamroch (2002), and in our preceding paper (2004), where we briefly review the maneuvering designs proposed in these references.

The general *maneuvering problem* is divided into a *geometric task* and a *dynamic task*. The geometric task, often referred to as *path following*, is to reach the path and then to stay on it, while the dynamic task specifies a time, speed, or acceleration assignment along the path. This is in contrast with the common *tracking problem* which merges the geometric and dynamic tasks into a single task with objectives often more stringent than required in applications.

The maneuvering problem formulation implies the existence of a forward invariant and globally attractive manifold to which all solutions must converge. The closed-loop system is correspondingly analyzed as a set-stability problem, for which the necessary mathematical tools are provided in Appendix A.

In our preceding paper, Skjetne, Fossen, and Kokotović (2004), are presented a maneuvering design robust to unknown bounded disturbances. In this paper, we present an adaptive version of the maneuvering methodology. The general design has been developed in Skjetne (2005) for nonlinear plants in vectorial parametric strict feedback

☆ This paper was not presented at any IFAC meeting. This paper was recommended for publication in revised form by Associate Editor A. Astolfi under the direction of Editor H.K. Khalil.
* Corresponding author. Tel.: +47 73594374; fax: +47 73594399.
E-mail addresses: skjetne@ieee.org (R. Skjetne), tif@itk.ntnu.no (T.I. Fossen), petar@ece.ucsb.edu (P.V. Kokotović).

0005-1098/$ - see front matter © 2004 Elsevier Ltd. All rights reserved.
doi:10.1016/j.automatica.2004.10.006

form (Krstić, Kanellakopoulos, & Kokotović, 1995) of any vector relative degree. For brevity, the constructive design procedure and analysis are performed solely in this paper for a model ship scaled to closely approximate its real-life original. The last section of the paper describes two experiments to verify the success of the design and to illustrate important performance features of two different controller implementations. While the familiarity with the preceding paper (2004) would be beneficial, this paper is self-contained and can be read without it.

Notation: Total time derivatives of $x(t)$ are denoted $\dot{x}$, $\ddot{x}$, $x^{(3)}, \ldots, x^{(n)}$, while a superscript denotes partial differentiation: $\alpha^t(x,\theta,t) := \partial\alpha/\partial t$, $\alpha^{x^2}(x,\theta,t) := \partial^2\alpha/\partial x^2$, and $\alpha^{\theta^n}(x,\theta,t) := \partial^n\alpha/\partial\theta^n$, etc. The Euclidean vector norm is $|x| := (x^\top x)^{1/2}$, and the distance to a set $\mathscr{M}$ is $|x|_{\mathscr{M}} := \inf\{|x-y| : y \in \mathscr{M}\}$. The max/min eigenvalues of A are $\lambda_{\max/\min}(A)$. Whenever convenient, $|(x,y,z)|$ indicates the norm of the vector $[x^\top, y^\top, z^\top]^\top$.

2. Case study: adaptive maneuvering of CyberShip II

The case study of maneuvering the model ship called CyberShip II (CS2; see Fig. 1) along a desired path is used to illustrate and experimentally test the adaptive maneuvering control design. CS2 is a 1:70 scale replica of a supply ship. Its mass is $m = 23.8\,\text{kg}$, its length is $L_{\text{CS2}} = 1.255\,\text{m}$, and its breadth is $B_{\text{CS2}} = 0.29\,\text{m}$. It is fully actuated with two main propellers and two rudders aft, and one bow thruster. It is further equipped with a PC104-bus driven by a QNX® real-time operating system which controls the internal hardware architecture and communicates with onshore computers through a WLAN in the Marine Cybernetics Laboratory (MCLab). This laboratory is a Marie Curie EU training site for testing of ships, rigs, underwater vehicles, and propulsion systems. It is equipped with a towing carriage, a wave maker system, and a measurement system that provides full state measurements. To facilitate real-time feedback control of the ship, Opal RT-Lab® is used for rapid prototyping of a desired control structure programmed in Matlab® and Simulink®. For execution of the experiment, a LabVIEW® interface has been developed for commanding and monitoring the ship.

Let $\eta = [x, y, \psi]^\top$ be the three DOF position (x, y) and heading (ψ) of the ship in an earth-fixed inertial frame, and let $v = [u, v, r]^\top$ be the corresponding linear velocities (u, v)—called surge and sway—and angular rate (r)—called yaw—in the body-fixed frame. According to Fossen (2002), the dynamic model of the ship is

$$\begin{aligned}\dot{\eta} &= R(\psi)v,\\ M\dot{v} &= \tau - C(v)v - D(v)v + R(\psi)^\top b.\end{aligned} \tag{1}$$

The vector $b = [b_1, b_2, b_3]^\top$, $\dot{b} = 0$, represents a constant (or slowly varying) unknown bias due to external environmental forces. $R(\cdot)$ is the three DOF rotation matrix with the properties that $R(\psi)^\top R(\psi) = I$, $\|R(\psi)\| = 1$ for all ψ, and $(\mathrm{d}/\mathrm{d}t)\{R(\psi)\} = \dot{\psi}R(\psi)S$ where

$$R(\psi) := \begin{bmatrix}\cos\psi & -\sin\psi & 0\\ \sin\psi & \cos\psi & 0\\ 0 & 0 & 1\end{bmatrix}, \quad S := \begin{bmatrix}0 & -1 & 0\\ 1 & 0 & 0\\ 0 & 0 & 0\end{bmatrix}.$$

The system inertia matrix $M = M^\top > 0$ is

$$M = \begin{bmatrix}m - X_{\dot{u}} & 0 & 0\\ 0 & m - Y_{\dot{v}} & mx_g - Y_{\dot{r}}\\ 0 & mx_g - N_{\dot{v}} & I_z - N_{\dot{r}}\end{bmatrix},$$

where $Y_{\dot{r}} = N_{\dot{v}}$, $C(v) = -C(v)^\top$ is a skew-symmetric matrix of Coriolis and centripetal terms,

$$C(v) = \begin{bmatrix}0 & 0 & c_{13}(v)\\ 0 & 0 & c_{23}(v)\\ -c_{13}(v) & -c_{23}(v) & 0\end{bmatrix}$$

with $c_{13}(v) = -(m - Y_{\dot{v}})v - (mx_g - Y_{\dot{r}})r$ and $c_{23}(v) = (m - X_{\dot{u}})u$, and $D(v)$ is a nonlinear damping matrix,

$$D(v) = \begin{bmatrix}d_{11}(v) & 0 & 0\\ 0 & d_{22}(v) & d_{23}(v)\\ 0 & d_{32}(v) & d_{33}(v)\end{bmatrix}$$

with $d_{11}(v) = -X_u - X_{|u|u}|u| - X_{uuu}u^2$, $d_{22}(v) = -Y_v - Y_{|v|v}|v| - Y_{|r|v}|r|$, $d_{23}(v) = -Y_r - Y_{|v|r}|v| - Y_{|r|r}|r|$, $d_{32}(v) = -N_v - N_{|v|v}|v| - N_{|r|v}|r|$, and $d_{33}(v) = -N_r - N_{|v|r}|v| - N_{|r|r}|r|$. The coefficients $\{X_{(\cdot)}, Y_{(\cdot)}, N_{(\cdot)}\}$ are hydrodynamic parameters according to the notation of The Society of Naval Architects and Marine Engineers (1950), see also Clarke (2003). The input $\tau = [\tau_u, \tau_v, \tau_r]^\top$ of generalized control forces and moments is related to the propeller revolutions $n = (n_1, n_2, n_3)$ and rudder angles $\delta = (\delta_1, \delta_2)$ through a nonlinear mapping

$$\tau = Bf_{\text{c}}(v, n, \delta),$$

where $B \in \mathbb{R}^{3\times 5}$ is an actuator configuration matrix and $f_{\text{c}} : \mathbb{R}^3 \times \mathbb{R}^3 \times [-\pi, \pi)^2 \to \mathbb{R}^5$ is a function that for each velocity v relates the actuator set-points (n, δ) to a vector of forces. Finding optimal actuator set-points (n, δ) for each commanded force τ is called control allocation (Johansen, Fossen, & Tøndel, 2005). For CS2 this has been developed by Lindegaard and Fossen (2003). Our control input is, therefore, τ for which the saturation limits are approximately $|\tau_u|, |\tau_v| \leqslant 2.0\,\text{N}$ and $|\tau_r| \leqslant 1.5\,\text{N m}$.

The coefficients in M (and therefore $C(v)$) are determined quite accurately using semi-empirical methods or hydrodynamic computation programs. The main difficulty is to find the coefficients in the damping matrix. By towing the ship at different speeds in different directions and measuring the corresponding drag forces, about half of them have been identified; see Table 1.

The uncertain constant parameter vector is then $\varphi := [Y_{|r|v}, Y_{|v|r}, Y_{|r|r}, N_{|v|v}, N_r, N_{|v|r}, N_{|r|r}, b_1, b_2, b_3]^\top \in \mathbb{R}^{10}$, and the ship dynamic equations are rewritten as

$$\begin{aligned}\dot{\eta} &= R(\psi)v,\\ M\dot{v} &= \tau - C(v)v + \kappa(v) + \Phi(\eta, v)\varphi,\end{aligned} \tag{2}$$

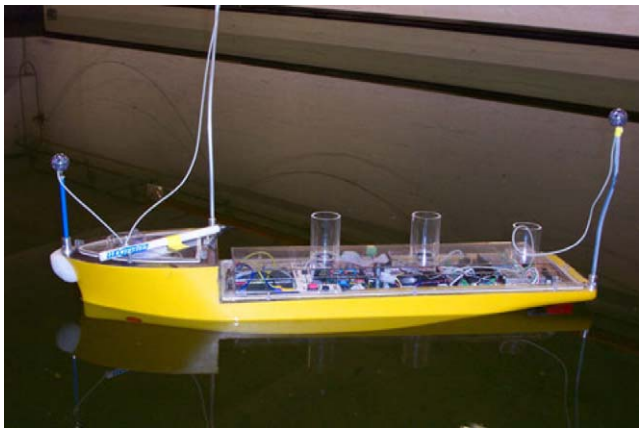

Fig. 1. A picture of CyberShip II in the Marine Cybernetics Laboratory (MCLab) at NTNU.

Table 1
A priori identified parameters for CS2

m	23.8000	Y_v	−0.8612	$X_{\dot{u}}$	−2.0
I_z	1.7600	$Y_{\|v\|v}$	−36.2823	$Y_{\dot{v}}$	−10.0
x_g	0.0460	Y_r	0.1079	$Y_{\dot{r}}$	−0.0
X_u	−0.7225	N_v	0.1052	$N_{\dot{v}}$	−0.0
$X_{\|u\|u}$	−1.3274	$N_{\|v\|v}$	5.0437	$N_{\dot{r}}$	−1.0
X_{uuu}	−5.8664				

where $\kappa(v)$ is the known part of $-D(v)v$ and

$$\Phi(\eta, v) := \begin{bmatrix} 0 & 0 & 0 & 0 & 0 & 0 & 0 & \cos\psi & \sin\psi & 0 \\ |r|v & |v|r & |r|r & 0 & 0 & 0 & 0 & -\sin\psi & \cos\psi & 0 \\ 0 & 0 & 0 & |r|v & r & |v|r & |r|r & 0 & 0 & 1 \end{bmatrix}$$

is the regressor matrix so that $\kappa(v) + \Phi(\eta, v)\varphi = R(\psi)^\top b - D(v)v$. Premultiplying by M^{-1}, model (2) is in parametric strict feedback form (Krstić et al., 1995).

2.1. Problem statement

In *maneuvering*, the main task is to converge to and follow a desired *parametrized path*. For the ship application, this means to converge to the geometric path

$$\eta_d(\theta) = [x_d(\theta), \quad y_d(\theta), \quad \psi_d(\theta)]^\top \tag{3}$$

continuously parametrized by the path variable θ. The second task is to satisfy a *desired dynamic behavior* along the path given as a specification on the speed of $\theta(t)$. This motivates the *Maneuvering Problem* (Skjetne et al., 2004), stated as:

1. *Geometric Task*: For any continuous function $\theta(t)$, force the ship to converge to and follow the desired path:

$$\lim_{t\to\infty} |\eta(t) - \eta_d(\theta(t))| = 0. \tag{4}$$

2. *Dynamic Task*: Force the path speed $\dot{\theta}$ to converge to the desired speed assignment $\upsilon_s(\theta, t)$:

$$\lim_{t\to\infty} |\dot{\theta}(t) - \upsilon_s(\theta(t), t)| = 0. \tag{5}$$

Assumption 2.1. The path $\eta_d(\theta)$ and its first and second partial derivatives are uniformly bounded on $\mathbb{R}^3$. The speed assignment $\upsilon_s(\theta, t)$ and its first partial derivatives are uniformly bounded in θ and t.

The explicit time dependence of $t \mapsto \upsilon_s(\theta, t)$, for all $t \geqslant t_0$, will make the closed-loop system time-varying. This has consequences for the later stability analysis. However, as shown by Teel and Praly (2000), a time-varying case can be subsumed into a time-invariant framework by treating time as an additional state with its own dynamics. For clarity, for this purpose we use the variable p, that is, the extended-state dynamic system will be composed of (2) and

$$\dot{p} = 1, \quad p(0) = t_0. \tag{6}$$

Correspondingly, the time variable for the new extended-state system will be denoted, as in Definition A.1, by t with initial time $t = 0$. Note that, in particular, $p(t) = t + t_0$ for all $t \geqslant 0$ and consequently[1] $\upsilon_s(\cdot, p)$ conforms to (5) for each $p \geqslant t_0$ and each corresponding $t \geqslant 0$.

Such a state augmentation is used in this paper to design a feedback control law for (2) to guarantee that in the space of $(\eta, v, \hat{\varphi}, \theta, p) \in \mathbb{R}^3 \times \mathbb{R}^3 \times \mathbb{R}^{10} \times \mathbb{R} \times \mathbb{R}_{\geqslant 0}$ the closed-loop system possesses a globally attractive manifold, where $\hat{\varphi}$ denotes the dynamic estimate of φ. The expression for the desired manifold is obtained by differentiating $\eta = \eta_d(\theta)$ along the solutions of (2) with $\dot{\theta} = \upsilon_s(\theta, p)$, which gives

$$\mathscr{E} := \{\eta = \eta_d(\theta), v = R(\psi_d(\theta))^\top \eta_d^\theta(\theta)\upsilon_s(\theta, p)\}. \tag{7}$$

Clearly, every solution in $\mathscr{E}$ satisfies the geometric task (4). To see that it also satisfies the dynamic task (5), we differentiate $\eta_d(\theta) \equiv \eta$ to get $\eta_d^\theta(\theta)\dot{\theta} = \dot{\eta} = R(\psi)v = R(\psi_d(\theta))R(\psi_d(\theta))^\top \eta_d^\theta(\theta)\upsilon_s(\theta, p) = \eta_d^\theta(\theta)\upsilon_s(\theta, p)$, which holds for all (θ, p) and thus shows[2] that $\dot{\theta} = \upsilon_s(\theta, p)$ in $\mathscr{E}$.

The manifold $\mathscr{E}$ is unbounded in the directions of θ and p. The maneuvering problem is, therefore, recast in the framework of set-stability for closed, forward invariant sets. Denoting $\tilde{\varphi} := \varphi - \hat{\varphi}$ the error between the parameter vector φ and its estimate $\hat{\varphi}$, the adaptive backstepping procedure presented in the next section will recursively construct a global diffeomorphism into new error coordinates $z = [z_1^\top, z_2^\top]^\top \in \mathbb{R}^6$, $z = \Psi(\eta, v, \theta, p)$ such that $z = 0$ if

[1] Since the explicit time-variation only enters through the design function $\upsilon_s(\theta, \cdot)$, we could in principle define a new state p, running inside the control computer with dynamics $\dot{p} = 1$, $p(0) = t_0$, in order to implement t. This would indeed make the closed-loop system time-invariant. There is, however, no quantitative difference in this as compared to just using time t, for $t \geqslant t_0$, directly.

[2] Except for the case $\eta_d^\theta(\theta) \equiv 0$ when the path $\eta_d(\theta)$ is reduced to a fixed point.

and only if $(\eta, v, \hat{\varphi}, \theta, p) \in \mathscr{E}$. By including the constraint $\tilde{\varphi} = 0$, the desired set then becomes the closed, noncompact subset, $\mathscr{M} \subset \mathscr{E}$, given as

$$\mathscr{M} := \{(\eta, v, \hat{\varphi}, \theta, p): \Psi(\eta, v, \theta, p) = 0, \hat{\varphi} - \varphi = 0\}. \quad (8)$$

The resulting control law presented in the next section will ensure global attractivity of $\mathscr{E}$, while rendering $\mathscr{M}$ *uniformly globally stable* (UGS) according to Definition A.1.

2.2. Adaptive maneuvering control design

The design follows the recursive procedure of Krstić et al. (1995) with the distinction made between the notions of a *tuning function* and an *adaptive tuning function.*

Step 1: Define the error variables

$$z_1(\eta, \theta) := R(\psi)^\top(\eta - \eta_d(\theta)), \quad (9)$$
$$z_2(v, \eta, \theta, p) := v - \alpha_1(\eta, \theta, p), \quad (10)$$
$$\omega_s(\dot{\theta}, \theta, p) := \upsilon_s(\theta, p) - \dot{\theta}, \quad (11)$$
$$\tilde{\varphi} := \varphi - \hat{\varphi}, \quad (12)$$

where $\hat{\varphi}$ is the parameter estimate and α_1 is a *virtual control* to be specified later. Observe that z_1 is decomposed in the body-fixed ship frame. This means that the controller gains will not depend on the ship heading, a common trick in vessel control (Lindegaard & Fossen, 2003) used to aid the tuning process. Differentiating (9) with respect to time yields

$$\begin{aligned}\dot{z}_1 &= \dot{R}(\psi)^\top(\eta - \eta_d(\theta)) + R(\psi)^\top(\dot{\eta} - \eta_d^\theta(\theta)\dot{\theta}) \\ &= -rSz_1 + z_2 + \alpha_1 - R(\psi)^\top\eta_d^\theta(\theta)\dot{\theta}, \end{aligned} \quad (13)$$

where we used $R(\psi)^\top R(\psi) = I$ and $\dot{R}(\psi) = rR(\psi)S$. Define the first control Lyapunov function (CLF) as

$$V_1(z_1) := \tfrac{1}{2} z_1^\top z_1 \quad (14)$$

whose time derivative is

$$\dot{V}_1 = z_1^\top[\alpha_1 - R(\psi)^\top\eta_d^\theta\upsilon_s] + z_1^\top z_2 + z_1^\top R(\psi)^\top\eta_d^\theta\omega_s$$

due to skew-symmetry of $S = -S^\top$, giving $z_1^\top S z_1 = 0$ for all z_1. With the virtual control law

$$\alpha_1 = \alpha_1(\eta, \theta, p) = -K_p z_1 + R(\psi)^\top\eta_d^\theta(\theta)\upsilon_s(\theta, p), \quad (15)$$

where $K_p = K_p^\top > 0$, and the first tuning function

$$\rho_1(\eta, \theta) := z_1^\top R(\psi)^\top\eta_d^\theta(\theta), \quad (16)$$

the result of Step 1 becomes

$$\dot{z}_1 = -K_p z_1 - rSz_1 + z_2 + R(\psi)^\top\eta_d^\theta(\theta)\omega_s, \quad (17)$$
$$\dot{V}_1 = -z_1^\top K_p z_1 + z_1^\top z_2 + \rho_1\omega_s \quad (18)$$

leaving the terms containing z_2 and ω_s for the next step. To aid the next step, let

$$\begin{aligned}\dot{\alpha}_1 &=: \sigma_1 + \alpha_1^\theta\dot{\theta}, \\ \sigma_1 &= -K_p(v - rSz_1) - rSR(\psi)^\top\eta_d^\theta(\theta)\upsilon_s(\theta, p) \\ &\quad + R(\psi)^\top\eta_d^\theta(\theta)\upsilon_s^p(\theta, p), \end{aligned} \quad (19)$$
$$\begin{aligned}\alpha_1^\theta &= K_p R(\psi)^\top\eta_d^\theta(\theta) + R(\psi)^\top[\eta_d^{\theta^2}(\theta)\upsilon_s(\theta, p) \\ &\quad + \eta_d^\theta(\theta)\upsilon_s^\theta(\theta, p)]. \end{aligned} \quad (20)$$

Step 2: Differentiating (10) with respect to time yields

$$\begin{aligned}M\dot{z}_2 &= M\dot{v} - M\dot{\alpha}_1 \\ &= \tau - C(v)v + \kappa(v) + \Phi(\eta, v)\varphi - M\sigma_1 - M\alpha_1^\theta\dot{\theta}, \end{aligned} \quad (21)$$

where $M = M^\top > 0$. Let $\Gamma = \Gamma^\top > 0$ and define the second CLF

$$V_2(z_1, z_2, \tilde{\varphi}) := V_1(z_1) + \tfrac{1}{2} z_2^\top M z_2 + \tfrac{1}{2}\tilde{\varphi}^\top\Gamma^{-1}\tilde{\varphi} \quad (22)$$

whose time derivative is

$$\begin{aligned}\dot{V}_2 &= \dot{V}_1 + z_2^\top M\dot{z}_2 - \tilde{\varphi}^\top\Gamma^{-1}\dot{\hat{\varphi}} \\ &= -z_1^\top K_p z_1 + (\rho_1 + z_2^\top M\alpha_1^\theta)\omega_s \\ &\quad + \tilde{\varphi}^\top[\Phi^\top z_2 - \Gamma^{-1}\dot{\hat{\varphi}}] \\ &\quad + z_2^\top[z_1 + \tau - Cv + \kappa + \Phi\hat{\varphi} - M\sigma_1 - M\alpha_1^\theta\upsilon_s], \end{aligned}$$

where $\Phi(\eta, v)^\top z_2$ is recognized as the *adaptive tuning function* (Krstić et al., 1995). The static part of the control law and the adaptive update law for $\hat{\varphi}$ are then designed as

$$\begin{aligned}\tau &= \alpha_2(\eta, v, \hat{\varphi}, \theta, p) \\ &= -z_1 - K_d z_2 + C\alpha_1 - \kappa - \Phi\hat{\varphi} + M\sigma_1 + M\alpha_1^\theta\upsilon_s, \end{aligned} \quad (23)$$
$$\dot{\hat{\varphi}} = \Gamma\Phi(\eta, v)^\top z_2, \quad (24)$$

where $K_d = K_d^\top > 0$. Defining the second tuning function

$$\begin{aligned}\rho_2(\eta, v, \theta, p) &:= \rho_1 + z_2^\top M\alpha_1^\theta \\ &= \eta_d^\theta(\theta)^\top R(\psi)z_1(\eta, \theta) \\ &\quad + \alpha_1^\theta(\eta, \theta, p)^\top M z_2(v, \eta, \theta, p) \end{aligned} \quad (25)$$

and taking into account $z_2^\top C(v)z_2 = 0$, $\forall z_2$, we get

$$\dot{V}_2 = -z_1^\top K_p z_1 - z_2^\top K_d z_2 + \rho_2\omega_s. \quad (26)$$

The global diffeomorphism

$$(\eta, v, \hat{\varphi}, \theta, p) \mapsto (z_1, z_2, \tilde{\varphi}, \theta, p)$$

is now explicitly given by $\tilde{\varphi} = \varphi - \hat{\varphi}$ and

$$\begin{aligned} z &= \Psi(\eta, v, \theta, p) \\ &:= \begin{bmatrix} R(\psi)^\top(\eta - \eta_d(\theta)) \\ K_p R(\psi)^\top(\eta - \eta_d(\theta)) + v - R(\psi)^\top\eta_d^\theta(\theta)\upsilon_s(\theta, p) \end{bmatrix} \end{aligned} \quad (27)$$

which is bounded in (θ, p) by Assumption 2.1. The resulting closed-loop system becomes

$$\begin{aligned}\dot{z} &= A_z(v)z + g(\eta, \theta, p)\omega_s + H\Phi(\eta, v)\tilde{\varphi},\\ \dot{\tilde{\varphi}} &= \Gamma\Phi(\eta, v)^\top M H^\top z,\\ \dot{\theta} &= \upsilon_s(\theta, p) - \omega_s,\end{aligned} \tag{28}$$

where

$$A_z := \begin{bmatrix} -K_p - rS & I \\ -M^{-1} & -M^{-1}(K_d + C(v)) \end{bmatrix}, \tag{29}$$

$$g := \begin{bmatrix} R(\psi)^\top \eta_d^\theta(\theta) \\ \alpha_1^\theta(\eta, \theta, p) \end{bmatrix}, \quad H := \begin{bmatrix} 0 \\ M^{-1} \end{bmatrix}. \tag{30}$$

Rendering the term $\rho_2\omega_s$ in (26) nonpositive for all $t \geqslant 0$ results in a negative semi-definite $\dot{V}_2$ and solves the Maneuvering Problem.

Theorem 2.2. *For the closed-loop system* (28), *every smooth function* $\omega_s = \omega(\eta, v, \hat{\varphi}, \theta, p)$, *bounded in* (θ, p) *such that*

(1) $\omega_s = 0$ *for all* $(\eta, v, \hat{\varphi}, \theta, p) \in \mathscr{E}$,
(2) $\rho_2(\eta(t), v(t), \theta(t), p(t))\omega_s(t) \leqslant 0, \quad \forall t \geqslant 0$, *renders* $\mathscr{E}$ *in* (7) *globally attractive and* $\mathscr{M}$ *in* (8) UGS.

Proof. For set (8), rewritten as

$$\begin{aligned}\mathscr{M} := \{&(z, \tilde{\varphi}, \theta, p) \in \mathbb{R}^6 \times \mathbb{R}^{10} \times \mathbb{R} \\ &\times \mathbb{R}_{\geqslant 0} : z = 0, \tilde{\varphi} = 0\},\end{aligned}$$

the distance function is $|(z, \tilde{\varphi}, \theta, p)|_{\mathscr{M}} = |(z, \tilde{\varphi})|$. Since $\mathscr{M} \subset \mathscr{E}$ we have that $\omega_s = 0$ in $\mathscr{M}$, and thus $\mathscr{M}$ is forward invariant for (28). Furthermore, (22) and (26) satisfy (A.4), (A.5) with $\gamma_1 := c_1|(z, \tilde{\varphi})|^2$, $\gamma_2 := c_2|(z, \tilde{\varphi})|^2$, and $\gamma_3 := c_3|z|^2$, where $c_1 := \frac{1}{2}\min\{1, \lambda_{\min}(M), \lambda_{\min}(\Gamma^{-1})\}$, $c_2 := \frac{1}{2}\max\{1, \lambda_{\max}(M), \lambda_{\max}(\Gamma^{-1})\}$, and $c_3 := \min\{1, \lambda_{\min}(K_p), \lambda_{\min}(K_d)\}$. Now, for each finite $K > 0$ such that $|(z, \tilde{\varphi}, \theta, p)|_{\mathscr{M}} = |(z, \tilde{\varphi})| \leqslant K$, it follows by Assumption 2.1 and (12), (27) that $(\eta, v, \hat{\varphi})$, and ω_s by continuity, are bounded. Hence, there exists, for each K, an upper bound $L > 0$ on the right-hand side of (28). By Theorem A.2 it follows that $\mathscr{M}$ is UGS with respect to (28), and $\gamma_3(|(z(t), \tilde{\varphi}(t), \theta(t), p(t))|_{\mathscr{M}}) = c_3|z(t)|^2 \to 0$ as $t \to \infty$ shows that $\mathscr{E}$ is globally attractive. □

2.3. Closing the loop by speed assignment designs

Satisfying the conditions of Theorem 2.2 for ω_s is accomodated by one of the choices, the *Tracking* or the *Gradient* update laws, as shown in Skjetne et al. (2004).

1. *Tracking update law*: Setting $\omega_s = 0$ satisfies the speed assignment (5) identically. The dynamic part of the control law becomes the time-varying reference system

$$\dot{\theta} = \upsilon_s(\theta, p), \tag{31}$$

which, through $\eta_d(\theta)$, sets the desired motion along the path.

2. *Gradient update law*: For $\mu \geqslant 0$, then $\omega_s = -\mu\rho_2(\eta, v, \theta, p)$ is bounded in (θ, p) by Assumption 2.1 and satisfies Theorem 2.2 since $\rho_2 = 0$ for $z = 0$. We call this a *Gradient* update law because

$$\rho_2 = -\frac{\partial V_2}{\partial \theta}(z_1(\eta, \theta), z_2(\eta, v, \theta, p), \tilde{\varphi}), \tag{32}$$

and the dynamic part of the control law becomes

$$\begin{aligned}\dot{\theta} &= \upsilon_s(\theta, p) + \mu\rho_2(\eta, v, \theta, p)\\ &= \upsilon_s(\theta, p) - \mu V_2^\theta(z_1(\eta, \theta), z_2(\eta, v, \theta, p), \tilde{\varphi}).\end{aligned} \tag{33}$$

Comparing the two update laws, it is noticed that $\mu = 0$ reduces (33)–(31). For $\mu \gg 0$ it was shown in Skjetne, Teel, and Kokotović(2002a,b) that the closed-loop system (28), using (33) with $\varepsilon := 1/\mu$, can be rewritten in *singular perturbation standard form* (Kokotović, Khalil, & O'Reilly, 1999). Letting $\varepsilon \to 0$, $\theta(t)$ rapidly converges to a value $\bar{\theta}(t)$ which yields a minimum of $V_2(z_1(\eta, \theta), z_2(\eta, v, \theta, p), \tilde{\varphi})$. In view of (14) and (22), the point $\eta_d(\bar{\theta}(t))$ minimizes the sum of the weighted squares of z_1 and z_2 with respect to θ. The distance to $\mathscr{E}$ will, therefore, always be kept at a minimum, with respect to θ, for μ large.

3. *Filtered-gradient update law*: A further possibility is to choose ω_s as an additional state and augment V_2 to

$$V = V_2 + \frac{1}{2\lambda\mu}\omega_s^2, \quad \lambda, \mu > 0. \tag{34}$$

In its derivative

$$\begin{aligned}\dot{V} &= \dot{V}_2 + \frac{1}{\lambda\mu}\omega_s\dot{\omega}_s\\ &= -z_1^\top K_p z_1 - z_2^\top K_d z_2 + \left[\rho_2 + \frac{1}{\lambda\mu}\dot{\omega}_s\right]\omega_s,\end{aligned}$$

the last term is rendered negative with

$$\dot{\omega}_s = -\lambda(\omega_s + \mu\rho_2(\eta, v, \theta, p)) \tag{35}$$

resulting in

$$\dot{V} = -z_1^\top K_p z_1 - z_2^\top K_d z_2 - \frac{1}{\mu}\omega_s^2. \tag{36}$$

It follows by Theorem A.2, for all $\lambda, \mu > 0$, that in the space of $(z, \tilde{\varphi}, \omega_s, \theta, p) \in \mathbb{R}^6 \times \mathbb{R}^{10} \times \mathbb{R} \times \mathbb{R} \times \mathbb{R}_{\geqslant 0}$ the set $\mathscr{M}' := \{z = 0, \omega_s = 0, \tilde{\varphi} = 0\}$ is UGS and $\mathscr{E}' := \{z = 0, \omega_s = 0\}$ is globally attractive for the closed-loop system (28) and (35).

We note that (35) is (32) filtered by $-\mu\lambda/(s + \lambda)$, and the dynamic part of the control law

$$\begin{aligned}\dot{\theta} &= \upsilon_s(\theta, p) - \omega_s,\\ \dot{\omega}_s &= -\lambda\omega_s + \lambda\mu V_2^\theta,\end{aligned} \tag{37}$$

is, therefore, called the *filtered gradient* update law, having similar performance properties as (33). The cut-off frequency λ is used to mitigate measurement noise versus bandwidth. In the noise-free case one can increase λ, and as

$\lambda \to \infty$ the solution for ω_s approaches $\omega_s = -\mu\rho_2(\eta, v, \theta, p)$ in which case (37) reduces to (33); see Skjetne et al. (2002b).

3. Experimental results

In the following we report the results of two experiments performed in the MCLab. In the first, we run an adaptive maneuvering system for CS2 according to the design in the previous sections. In the second experiment we compare the performance of using the gradient update law implementation versus the tracking update law when the forward thrust τ_u is forced to saturate.

In both experiments, the desired output path was an ellipsoid with heading along the tangent vector, i.e.

$$\eta_d(\theta) = [x_d(\theta), \quad y_d(\theta), \quad \psi_d(\theta)]^\top \tag{38}$$

where $x_d(\theta) = 6 + 5\cos((\pi/180)\theta)$, $y_d(\theta) = -0.5 + 2.5\sin((\pi/180)\theta)$, and $\psi_d(\theta) = \arctan(y_d^\theta(\theta)/x_d^\theta(\theta))$. The dynamic task is further specified to make the desired surge velocity adjustable online by the operator. This is solved according to the relationship

$$u_d(t) = \sqrt{x_d^\theta(\theta(t))^2 + y_d^\theta(\theta(t))^2}\,\upsilon_s(\theta(t), t), \quad \forall t \geqslant t_0,$$

which gives the speed assignment

$$\begin{aligned}
\upsilon_s(\theta, t) &= \frac{u_d(t)}{\sqrt{x_d^\theta(\theta)^2 + y_d^\theta(\theta)^2}},\\
\upsilon_s^\theta(\theta, t) &= \frac{-[x_d^\theta(\theta)x_d^{\theta^2}(\theta) + y_d^\theta(\theta)y_d^{\theta^2}(\theta)]}{[x_d^\theta(\theta)^2 + y_d^\theta(\theta)^2]^{3/2}}u_d(t),\\
\upsilon_s^t(\theta, t) &= \frac{\dot{u}_d(t)}{\sqrt{x_d^\theta(\theta)^2 + y_d^\theta(\theta)^2}},
\end{aligned} \tag{39}$$

for which according to the previous notation and analysis we should substitute the explicit 't' with 'p'.

3.1. CS2 experiment 1: adaptive maneuvering

For this experiment, the gradient update law was applied. The controller settings for the experiment were $K_p = \mathrm{diag}(0.2, 1.0, 0.5)$, $K_d = \mathrm{diag}(3, 10, 7)$, $\mu = 400$, and $\Gamma = \mathrm{diag}(2, 2, 2, 2, 2, 2, 2, 1, 1, 1)$. The initial condition for the parameter update was $\hat{\varphi}(0) = [0, 0, 0, 0, -0.5, 0, 0, 0, 0, 0]^\top$. The ship was first put to rest in dynamic positioning (zero speed) at $\eta_d(0)$ and then the ship was commanded online to move along the path with different desired surge velocities.

Fig. 2 shows how CS2 accurately traced the path on its first round along the ellipsoid. In the total run it did many rounds, and the upper plot in Fig. 3 shows the commanded surge velocity $u_d(t)$ and the resulting response $u(t)$. The lower plot shows the corresponding speed assignment $\upsilon_s(\theta(t), t)$ and the resulting response of $\dot{\theta}(t)$. Clearly, $\dot{\theta}(t)$ worked actively to satisfy its twofold objective between the speed assignment and the Lyapunov cost function minimization. The time series of the parameter estimates $\hat{\varphi}(t)$ are shown in Fig. 4. For the full-scale vessel, the commanded velocities $\{0.10, 0.15, 0.20\}$ (m/s) corresponds to $\{1.55, 2.32, 3.10\}$ (knots). This is within the speed domain of dynamical positioning for which this model ship is built.

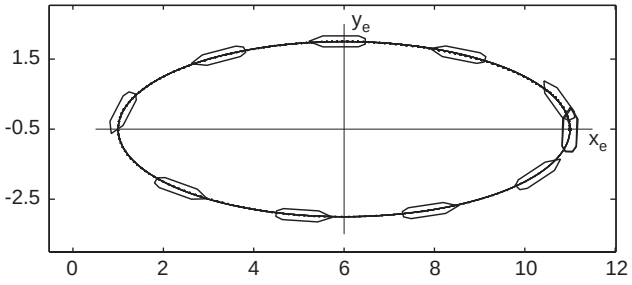

Fig. 2. Position response of CS2 following the desired ellipsoidal path in MC Lab, using an adaptive maneuvering control law with the gradient update law.

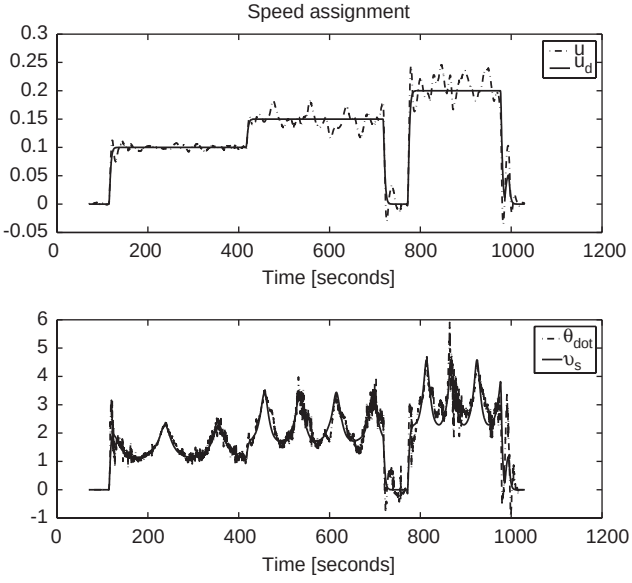

Fig. 3. Dynamic task: the upper plot shows the online commanded surge $u_d(t)$ and the resulting response of $u(t)$. The lower plot shows the corresponding speed assignment $\upsilon_s(\theta(t), t)$ and the resulting response of $\dot{\theta}(t)$.

Table 2 shows different standard deviations of error signals during the three different speed intervals. The most important variable for path keeping is z_{12} since this is an approximate measure of the cross-track error (provided the ship is pointed along the path). An accuracy of 2.42 cm in the highest speed corresponds to an accuracy of 1.69 m for the full-scale ship having a breadth of 20.3 m and is acceptable. We conclude that the adaptive maneuvering control law solved our control objective well.

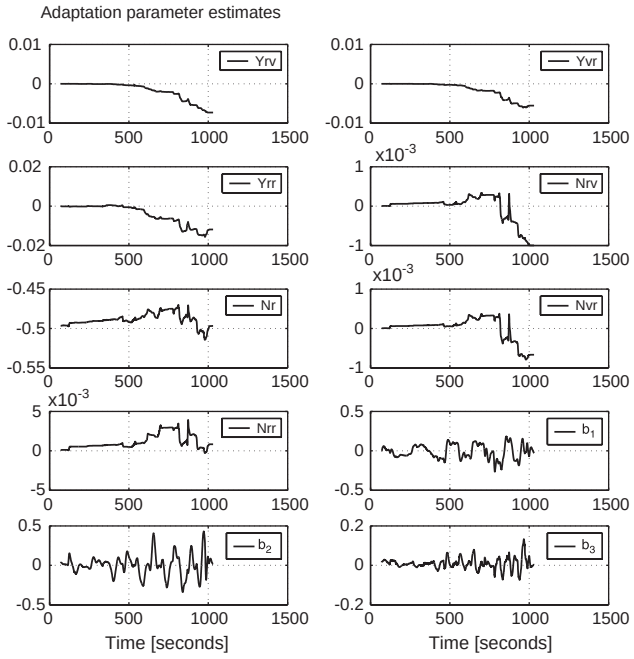

Fig. 4. The parameter estimates $\hat{\varphi}(t)$ in the first adaptive CS2 maneuvering experiment.

Table 2
Standard deviations for CS2 in the first experiment

u_d (m/s)	z_{11} (m)	z_{12} (m)	z_{13} (deg)	$u - u_d$ (m/s)
0.10	0.0118	0.0071	1.6358	0.0046
0.15	0.0377	0.0173	2.6319	0.0138
0.20	0.0567	0.0242	3.0466	0.0201

3.2. Ship experiment 2: tracking vs. gradient in a thrust failure scenario

In this experiment we compared the ship responses using the *tracking update law* and the *gradient update law* when the forward thrust τ_u cannot deliver enough force for the ship to track the commanded speed. To achieve this we induced the saturation limit $|\tau_u| \leqslant 0.1\,\mathrm{N}$ on the ship. The controller gains were the same as in the last experiment; however, for simplicity only the bias b was adapted so that $\Gamma = \mathrm{diag}(0, 0, 0, 0, 0, 0, 0, 1, 1, 1)$ with $\hat{\varphi}(0)$ initialized as before.

In both the cases, CS2 was first positioned at $\eta_d(0)$, then commanded for one round with $u_d = 0.10\,\mathrm{m/s}$, and when $\theta \approx 360°$ the commanded speed was changed to $u_d = 0.20\,\mathrm{m/s}$. The ship was tracing the path unproblematically at the speed $u_d = 0.10\,\mathrm{m/s}$ in both the tracking and gradient cases. However, when u_d changed to 0.20 m/s the closed-loop systems started to experience problems, as seen in the position responses for the second round in Fig. 5. While, not surprisingly, the tracking system soon went unstable, it was observed that the gradient-based system kept moving

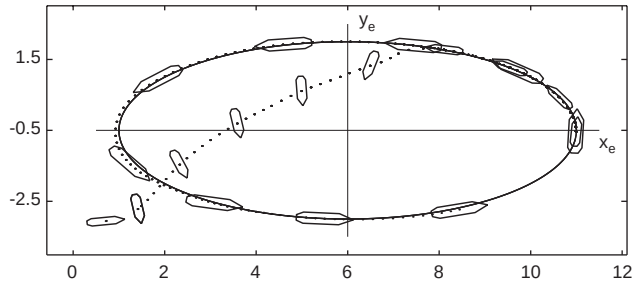

Fig. 5. Position responses using a tracking update law (small ship) and a gradient update law (large ship) in the second ship experiment with commanded speed $u_d = 0.20\,\mathrm{m/s}$. Both responses are superimposed in the same plot. Since CS2 cannot move with $u_d = 0.20\,\mathrm{m/s}$ under the induced saturation limit, the tracking-based system went unstable. The gradient-based system, on the other hand, safely maneuvered CS2 along the path, but at a slower speed.

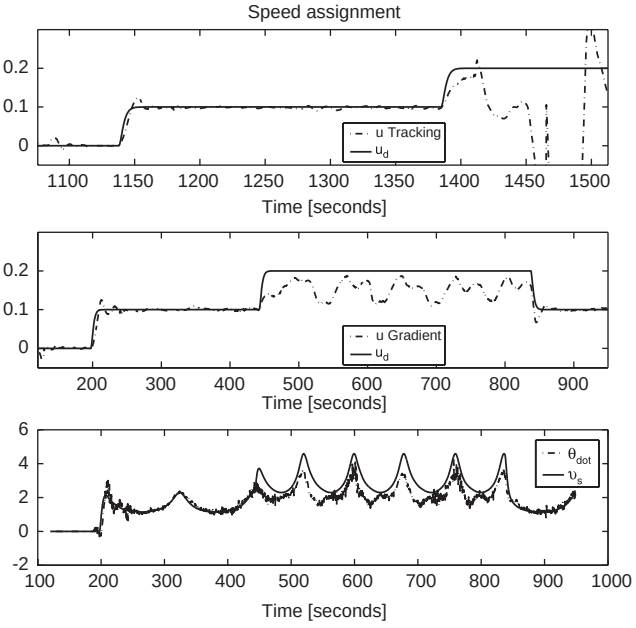

Fig. 6. Dynamic task: upper plot shows the commanded surge and resulting speed response for the tracking-based system, while the middle plot shows the same for the gradient-based system. Both systems satisfied the maneuvering objective well when $u_d = 0.10\,\mathrm{m/s}$, but the tracking-based system went unstable when u_d changed to 0.20 m/s. The lower plot shows $\upsilon_s(\theta(t), t)$ and $\dot{\theta}(t)$ for the gradient-based system only.

along the path, but with a speed slower than the infeasible $u_d = 0.20\,\mathrm{m/s}$. The lower plot in Fig. 6 reveals some of the secrets. While the speed assignment $\upsilon_s(\theta(t), t)$ strictly corresponds to the specified speed $u_d(t)$ according to (39), the response for $\dot{\theta}(t)$ was modified by the gradient term in the update law (see Skjetne et al., 2002a), trying to minimize the errors z_1 and z_2, and $\dot{\theta}(t)$, therefore, tracked a slower value. The result was that $\theta(t)$, and thus $\eta_d(\theta(t))$, moved not faster than the ship was able to follow.

This last experiment served to illustrate one of the advantages of using the gradient minimization feature in the

gradient or filtered-gradient update laws, as compared to using the pure tracking update law.

4. Conclusion

The *Maneuvering Problem* was defined as solving a *Geometric Task* and a *Dynamic Task*. The geometric task was to converge to and stay on a desired parametrized path, and the dynamic task was to satisfy a desired dynamic behavior along the path, here specified as a speed assignment. It was shown that this problem implied the existence of a non-compact attractive manifold in the state space to which the solutions had to converge.

An adaptive design procedure was applied in a case study to solve the maneuvering problem for a parametrically uncertain ship model. The design was finalized by constructing a dynamic control law using a *tracking*, *gradient*, or *filtered-gradient* update law. The procedure was experimentally tested for a real model ship in a marine control laboratory. The ability to adjust online the forward speed of the ship along the path was easily achieved by constructing the speed assignment properly. To highlight the performance property of the feedback in the gradient update law, a comparison between a tracking-based controller and a gradient-based controller was performed, and significant results were obtained in the event of a saturation failure in the ship.

Acknowledgements

The work has been supported by the Norwegian Research Council through the Strategic University Program on Marine Control and by the National Science Foundation under the Grant ECS-0228864.

Appendix A. Set-stability tools

Consider the nonlinear system

$$\dot{x} = f(x), \tag{A.1}$$

where for each $t \geqslant 0$, $x(t) \in \mathbb{R}^n$, and f is smooth. For each initial condition $x_0 = x(0)$, let $x(t, x_0)$ denote the solution defined on its maximal interval of existence $[0, T)$. The system is said to be *forward complete* if the solution exists for all $t \geqslant 0$ so that $T = +\infty$.

Definition A.1. If system (A.1) is forward complete, then for this system, a closed forward invariant set $\mathscr{A} \subset \mathbb{R}^n$ is:

- UGS if there exists a class-$\mathscr{K}_\infty$ function φ such that, $\forall x_0 \in \mathbb{R}^n$, the solution $x(t, x_0)$ satisfies

$$|x(t, x_0)|_{\mathscr{A}} \leqslant \varphi(|x_0|_{\mathscr{A}}), \quad \forall t \geqslant 0. \tag{A.2}$$

- UGAS if there exists a class-$\mathscr{KL}$ function β such that, $\forall x_0 \in \mathbb{R}^n$, the solution $x(t, x_0)$ satisfies

$$|x(t, x_0)|_{\mathscr{A}} \leqslant \beta(|x_0|_{\mathscr{A}},\ t), \quad \forall t \geqslant 0. \tag{A.3}$$

See Khalil (2002) for the definitions of $\mathscr{K}$, $\mathscr{K}_\infty$, and $\mathscr{KL}$ functions. Systems that are only UGS with respect to a set may also possess certain convergence properties. Closed-loop adaptive systems are often of this type. A convenient tool for analyzing such systems is a theorem due to LaSalle and Yoshizawa (see Krstić et al., 1995, Theorem 2.1) which we now extend to set-stability problems.

Theorem A.2. *Let a closed set $\mathscr{A} \subset \mathbb{R}^n$ be a forward invariant set for* (A.1). *Suppose for each $K \in [0, \infty)$ there exists $L \in [0, \infty)$ such that $|x|_{\mathscr{A}} \leqslant K \Rightarrow |f(x)| \leqslant L$. Then, if there exists a smooth function $V : \mathbb{R}^n \to \mathbb{R}_{\geqslant 0}$ such that*

$$\gamma_1(|x|_{\mathscr{A}}) \leqslant V(x) \leqslant \gamma_2(|x|_{\mathscr{A}}), \tag{A.4}$$

$$\dot{V} = V^x(x) f(x) \leqslant -\gamma_3(|x|_{\mathscr{A}}) \leqslant 0, \tag{A.5}$$

$\forall x \in \mathbb{R}^n$, where $\gamma_1, \gamma_2 \in \mathscr{K}_\infty$ and γ_3 is a continuous positive semidefinite function, then $\mathscr{A}$ is UGS *for* (A.1) *and*

$$\lim_{t\to\infty} \gamma_3(|x(t, x_0)|_{\mathscr{A}}) = 0. \tag{A.6}$$

Proof. Integration of (A.5) and the bounds (A.4) imply that for each $x_0 \in \mathbb{R}^n$ there exists $K \geqslant 0$ such that

$$\begin{aligned} |x(t, x_0)|_{\mathscr{A}} &\leqslant \gamma_1^{-1}(V(x(t, x_0))) \leqslant \gamma_1^{-1}(V(x_0)) \\ &\leqslant \gamma_1^{-1}(\gamma_2(|x_0|_{\mathscr{A}})) = \varphi(|x_0|_{\mathscr{A}}) \leqslant K, \end{aligned} \tag{A.7}$$

holds for all t in the maximal interval of existence $[0, T)$, where $\varphi(\cdot) := \gamma_1^{-1}(\gamma_2(\cdot)) \in \mathscr{K}_\infty$ is independent of T. The bound (A.7) implies there exists $L > 0$ such that integration of $|f(x(t, x_0))| \leqslant L$ along the solutions of (A.1) gives

$$|x(t, x_0) - x_0| \leqslant \int_0^t |f(x(s))|\, \mathrm{d}s \leqslant Lt,$$

$\forall t \in [0, T)$, excluding finite escape time so that $T = \infty$. Hence, UGS follows directly from (A.7). Since V is nonincreasing and bounded from below by zero, it has a limit V_∞ as $t \to \infty$. Integrating (A.5) gives

$$\begin{aligned} \lim_{t\to\infty} \int_0^t \gamma_3(|x(s, x_0)|_{\mathscr{A}})\, \mathrm{d}s &\leqslant -\lim_{t\to\infty} \int_0^t \dot{V}(x(s, x_0))\, \mathrm{d}s \\ &= \lim_{t\to\infty} \{V(x_0) - V(x(t, x_0))\} \\ &= V(x_0) - V_\infty, \end{aligned}$$

which is finite. We next show that $t \mapsto \gamma_3(|x(t, x_0)|_{\mathscr{A}})$ is uniformly continuous on $\mathbb{R}_{\geqslant 0}$. For each $\varepsilon > 0$ we let $\delta := \varepsilon/L$, and for any $t_1, t_2 \in \mathbb{R}_{\geqslant 0}$ with $|t_2 - t_1| \leqslant \delta$ we get

$$\begin{aligned} |x(t_2, x_0) - x(t_1, x_0)| &\leqslant \int_{t_1}^{t_2} |f(x(s, x_0))|\, \mathrm{d}s \\ &\leqslant L|t_2 - t_1| \leqslant \varepsilon, \end{aligned}$$

which shows that $x(t, x_0)$ is uniformly continuous. Next,

$$\begin{aligned} ||x|_{\mathscr{A}} - |y|_{\mathscr{A}}| &= \left| \inf_{v\in\mathscr{A}} |x - v| - \inf_{w\in\mathscr{A}} |y - w| \right|, \\ &\leqslant ||x - s| - |y - s||, \quad s \in \mathscr{A}, \\ &\leqslant |x - y|, \quad \forall x, y \in \mathbb{R}^n, \end{aligned}$$

shows that $|\cdot|_{\mathscr{A}}$ is globally Lipschitz and uniformly continuous. Finally, since $\gamma_3(\cdot)$ is continuous, it is uniformly continuous on the compact set $\{s \in \mathbb{R}_{\geqslant 0} : s \leqslant K\}$. Putting this together we conclude that $t \mapsto \gamma_3(|x(t, x_0)|_{\mathscr{A}})$ is uniformly continuous, and $\lim_{t\to\infty}\gamma_3(|x(t, x_0)|_{\mathscr{A}}) = 0$ follows from Barbalat's Lemma (Khalil, 2002, Lemma 8.2).

References

Al-Hiddabi, S., & McClamroch, N. (2002). Tracking and maneuver regulation control for nonlinear nonminimum phase systems: application to flight control. *IEEE Transactions on Control System Technology*, *10*(6), 780–792.

Clarke, D. (2003). The foundations of steering and manoeuvering. *Proceedings of the IFAC conference on manoeuvering and controlling marine crafts*, IFAC, Girona, Spain.

Encarnação, P., & Pascoal, A. (2001). Combined trajectory tracking and path following for marine craft. *Proceedings of the Mediterranean conference on control and automation*, Dubrovnik, Croatia.

Fossen, T. I. (2002). *Marine control systems: guidance, navigation, and control of ships, rigs and underwater vehicles*. Trondheim, Norway: Marine Cybernetics.

Hauser, J., & Hindman, R. (1995). Maneuver regulation from trajectory tracking: feedback linearizable systems. *Proceedings of the IFAC symposium on nonlinear control systems design* (pp. 595–600). IFAC, Lake Tahoe, CA, USA.

Hauser, J., & Hindman, R. (1997). Aggressive flight maneuvers. *Proceedings of the 36th IEEE conference on decision & control* (pp. 4186–4191). IEEE, San Diego, CA, USA.

Johansen, T. A., Fossen, T. I., & Tøndel, P. (2005). Efficient optimal constrained control allocation via multi-parametric programming. *AIAA Journal on Guidance and Dynamics*, *28*.

Khalil, H. K. (2002). *Nonlinear systems* (3rd ed.), Englewood Cliffs, NJ: Prentice-Hall Inc.

Kokotović, P., Khalil, H. K., & O'Reilly, J. (1999). Analysis and design. *Singular perturbation methods in control*. Philadelphia, PA: Society for Industrial and Applied Mathematics (SIAM), (corrected reprint of the 1986 original).

Krstić, M., Kanellakopoulos, I., & Kokotović, P. (1995). *Nonlinear and adaptive control design*. New York: Wiley.

Lindegaard, K.-P., & Fossen, T. I. (2003). Fuel efficient rudder and propeller control allocation for marine craft: experiments with a model ship. *IEEE Transactions on Control System Technology*, *11*(6).

Micaelli, A., & Samson, C. (1993). *Trajectory tracking for unicycle-type and two-steering-wheels mobile robots*. Research report 2097. Inst. National de Recherche en Informatique et en Automatique.

Pettersen, K. Y., & Lefeber, E. (2001). Way-point tracking control of ships. *Proceedings of the 40th IEEE conference on decision & control* (pp. 940–945). IEEE, Orlando, FL, USA.

Skjetne, R. (2005). *The maneuvering problem*. Ph.D. thesis, Norwegian University of Science & Technology, Trondheim, Norway.

Skjetne, R., Fossen, T. I., & Kokotović, P. V. (2004). Robust output maneuvering for a class of nonlinear systems. *Automatica*, *40*(3), 373–383.

Skjetne, R., Teel, A. R., & Kokotović, P. V. (2002a). Nonlinear maneuvering with gradient optimization. *Proceedings of the 41st IEEE conference on decision & control* (pp. 3926–3931). IEEE, Las Vegas, USA.

Skjetne, R., Teel, A. R., & Kokotović, P. V. (2002b). Stabilization of sets parametrized by a single variable: application to ship maneuvering. *Proceedings of the 15th international symposium on mathematical theory of networks and systems*. Notre Dame, IN, USA.

Teel, A. R., & Praly, L. (2000). A smooth Lyapunov function from a class-$\mathscr{KL}$ estimate involving two positive semidefinite functions. *ESAIM: Control, Optimisation and Calculus of Variations*, *5*, 313–367.

The Society of Naval Architects and Marine Engineers (1950). Nomenclature for treating the motion of a submerged body through a fluid, Technical and Research Bulletin No. 1–5.

Roger Skjetne received in 2000 his B.S. and M.S. degrees in electrical and computer engineering from the University of California at Santa Barbara with emphasis on control theory. He has recently finished his Ph.D. degree at the Norwegian University of Science and Technology at the Department of Engineering Cybernetics. His research interests are within general nonlinear control theory for maneuvering dynamical systems with applications toward guidance, navigation, and control of ocean vehicles.
Prior to his studies, he worked as an electrician for Aker Elektro in Norway on numerous oil installations in the North Sea. Presently, he is working for the company Marine Cybernetics on developing tools and procedures for testing and verification of safety-critical control systems for the maritime industry. He is a member of the IEEE, the Society of Naval Architects and Marine Engineers (SNAME), the Norwegian Society of Chartered Engineers, and the honor societies Tau Beta Pi and the Golden Key.

Professor Thor I. Fossen received the M.Sc. degree in *Naval Architecture* in 1987 from the Norwegian University of Science and Technology (NTNU) and the Ph.D. in *Engineering Cybernetics* from NTNU in 1991. In the period 1989–1990 he pursued postgraduate studies as a *Fulbright Scholar* in aerodynamics and flight control at the Department of Aero- and Astronautics, University of Washington, Seattle. In 1993 Fossen was appointed as a Professor of Guidance, Navigation and Control at NTNU. He is the author of the books "*Guidance and Control of Ocean Vehicles*" (John Wiley & Sons, 1994), "*Marine Control Systems*" (Marine Cybernetics, 2002) and co-author of the book "*New Directions in Nonlinear Observer Design*" (Springer Verlag, 1999). Fossen has served as principal supervisor to 15 Ph.D. students. He has been the IPC chair of the IFAC CAMS'95 and NOC chair CAMS'98, the chair of the IEEE of the Oceanic Engineering/Control Systems Chapter of the Norway Section (1996–2000) and he has served as the Vice Chair of the IFAC Technical Committee on Marine Systems (1995–1999). Fossen has been a key person in the development of the ABB dynamic positioning (DP) and autopilot systems. Fossen has also been involved in the design of the SeaLaunch trim and heel correction systems. His work on weather optimal positioning control for marine vessels received the Automatica Prize Paper Award in 2002. Fossen is currently one of the key scientists at the Centre for Ships and Ocean Structures (CESOS)-Norwegian Centre of Excellence.

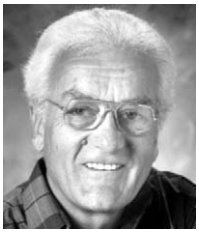

Petar V. Kokotovic has been active for four decades as control engineer, researcher, and educator, first in his native Yugoslavia and then, from 1966 through 1990, at the University of Illinois, where he held the endowed Grainger Chair. In 1991 he joined the University of California, Santa Barbara where he directed the Center for Control Engineering and Computation. He has co-authored eight books and numerous articles contributing

to sensitivity analysis, singular perturbation methods, and robust adaptive and nonlinear control. Professor Kokotovic is also active in industrial applications of control theory. As a consultant to Ford he was involved in the development of the first series of automotive computer controls and at General Electric he participated in large-scale systems studies. Professor Kokotovic is a Fellow of IEEE, and a member of National Academy of Engineering, USA. He received the 1983 and 1993 Outstanding IEEE Transactions Paper Awards and presented the 1991 Bode Prize Lecture. He is the recipient of the 1990 IFAC Quazza Medal, the 1995 IEEE Control Systems Award, the 2002 IEEE James H. Mulligan Jr. Education Medal, and the 2002 ACC Richard E. Bellman Control Heritage Award.